

Domain-wall fermions with U(1) dynamical gauge fields

S. Aoki and K. Nagai

Institute of Physics, University of Tsukuba, Tsukuba, Ibaraki 305, Japan

(Received 10 August 1995; revised manuscript received 22 January 1996)

We carry out a numerical simulation of a toy domain-wall model in $2+1$ dimensions, in the presence of a U(1) dynamical gauge field only in an extra dimension, corresponding to the weak coupling limit of a (two-dimensional) physical gauge coupling. Using a quenched approximation we investigate this model at $\beta_s (=1/g_s^2) = 0.5$ ("symmetric" phase), 1.0, and 5.0 ("broken" phase), where g_s is the gauge coupling constant of the extra dimension. In the broken phase, we find that there exists a critical value of the domain-wall mass m_0^c which separates a region with a fermionic zero mode on the domain wall from one without it. In the symmetric phase the critical value of the domain wall mass seems to exist but is very close to its upper bound $m_0 = 1$. Because of the difficulty observed in the numerical simulation near $m_0 = 1$ we cannot conclude in the symmetric phase either the existence of the chiral zero mode at $m_0 \geq m_0^c$ or the realization of the layered phase. [S0556-2821(96)06209-1]

PACS number(s): 11.15.Ha, 11.30.Rd

I. INTRODUCTION

Construction of chiral gauge theories is one of the long-standing problems of lattice field theories. Because of fermion doubling problems, a naively discretized lattice fermion field yields 2^d fermion particles, half of one chirality and half of the other, so that the theory becomes nonchiral [1]. Several lattice approaches have been proposed, but so far none of them have been proven to work successfully.

Kaplan has proposed a new construction of lattice chiral gauge theories via domain-wall models [2]. Starting from a vectorlike gauge theory in $2k+1$ dimensions with a fermion mass term being the shape of a domain wall in the (extra) $(2k+1)$ th dimension, he showed in the weak gauge coupling limit that a massless chiral state arises as a zero mode bound to the $2k$ -dimensional domain wall while all the doublers have large masses of the lattice cutoff scale. It has been also shown that the model works well for smooth background gauge fields [3–5].

Two simplified variants of the original Kaplan domain-wall model have been proposed: an "overlap formula" [6,7] and a "waveguide model" [8,9]. Gauge fields appearing in these variants are $2k$ dimensional and are independent of the extra $(2k+1)$ th coordinate, while those in the original model are $2k+1$ dimensional and depend on the extra $(2k+1)$ th coordinate. These variants work successfully for smooth background gauge fields [10–12], as the original one does. Nonperturbative investigations for these variants seem easier than for the original model due to the simpler structure of the gauge fields.

However, it has been reported [8,9] that the waveguide model in the weak gauge coupling limit cannot produce the chiral zero modes needed to construct chiral gauge theories. In this limit, if gauge invariance were maintained, pure gauge field configurations equivalent to unity by gauge transformation would dominate and gauge fields would become smooth. In the setup of the waveguide model, however, $2k$ -dimensional gauge fields are nonzero only in the layers near the domain wall (waveguide), so that gauge invariance is broken at the edge of the waveguide. Therefore, even in

the weak gauge coupling limit, gauge fields are no longer smooth and become very "rough," due to the gauge degrees of freedom appearing to be dynamical at this edge. As a result of the rough gauge dynamics, a new chiral zero mode with opposite chirality to the original zero mode on the domain wall appears at the edge, so that the fermionic spectrum inside the waveguide becomes vector like. It has been claimed [8,9] that this "rough gauge" problem also exists in the overlap formula since gauge invariance is broken by the boundary condition at the infinity of the extra dimension [11,12]. Furthermore, an equivalence between the waveguide model and the overlap formula has been pointed out for the special case [13]. Although the claimed equivalence has been challenged in Ref. [14], it is still crucial for the success of the overlap formula to solve the "rough gauge" problem and to show the existence of a chiral zero mode in the weak gauge coupling limit.

How about Kaplan's original model? In this model there are two inverse gauge couplings $\beta = 1/g^2$ and $\beta_s = 1/g_s^2$, where g is the coupling constant in (physical) $2k$ dimensions and g_s is the one in the (extra) $(2k+1)$ th dimension. Very little is known about this model except in the $\beta_s = 0$ case [8,15,16] where the spectrum seems vector like. Since perturbation theory for the physical gauge coupling g is expected to hold, the fermion spectrum of the model can be determined in the limit that $g \rightarrow 0$. In this weak coupling limit, all gauge fields in physical dimensions can be gauged away, while the gauge field in the extra dimension is still dynamical and its dynamics is controlled by β_s . Instead of the gauge degrees of freedom at the edge of the waveguide, the $(2k+1)$ th component of gauge fields represents the roughness of $2k$ -dimensional gauge fields. An important question is whether the chiral zero mode on the domain wall survives in the presence of this rough dynamics. The dynamics of the gauge field in this limit is equivalent to a $2k$ -dimensional scalar model with $2L_s$ independent copies where $2L_s$ is the number of sites in the extra dimension. In general at large β_s such a system is in a "broken phase" where some global symmetry is spontaneously broken, while at small β_s the system is in a "symmetric" phase. Therefore

there exists a critical point β_s^c , and it is likely that the phase transition at $\beta_s = \beta_s^c$ is continuous (second or higher order). The ‘‘gauge field’’ becomes rougher and rougher at smaller β_s . Indeed we know that the zero mode disappears at $\beta_s = 0$ [15], while the zero mode exists at $\beta_s = \infty$ (free case). So far we do not know the fate of the chiral zero mode in the intermediate range of the coupling β_s . There are the following three possibilities. (a) The chiral zero mode always exists except $\beta_s = 0$. In this case we may likely construct a lattice chiral gauge theory in both broken ($\beta_s > \beta_s^c$) and symmetric ($\beta_s < \beta_s^c$) phases, and the continuum limits may be taken at $\beta_s = \beta_s^c$. This is the best case for the domain-wall model. (b) The chiral zero mode exists only in the broken phase ($\beta_s > \beta_s^c$). In this case the domain-wall method can describe a lattice chiral gauge theory in the broken phase at finite cutoff. However, it is likely that the continuum limit taken at $\beta_s = \beta_s^c$ from above leads to a vector gauge theory. (c) No chiral zero mode survives except $\beta_s = \infty$. The original model cannot describe lattice chiral gauge theories at all.

It is very important to determine which possibility is indeed realized in the domain-wall model. Therefore, in this paper, in order to know the fate of the chiral zero mode, we carry out a numerical simulation of a domain-wall model in $(2+1)$ dimensions with a quenched U(1) gauge field in the $\beta_s = \infty$ limit. Strictly speaking, there is no order parameter in a two-dimensional U(1) spin model (XY model). On a large but finite lattice, however, the behavior of the two-dimensional model is similar to the one of a four-dimensional scalar model. Thus, we hopefully think that useful information about the fate of the zero mode can be obtained from such a toy model in $2+1$ dimensions. In Sec. II, we define our domain-wall model with dynamical gauge fields. We calculate a fermion propagator by using a kind of mean-field approximation, to show that there is a critical value of the domain-wall mass parameter above which the zero mode exist. The value of the critical mass may depend on β_s , which controls the dynamics of the gauge field. In Sec. III, we calculate the fermion spectrum numerically using a quenched approximation at $\beta_s = 0.5, 1.0, 5.0$ and at various values of domain-wall masses. We find that in the broken phase ($\beta_s = 1.0, 5.0$) there exists a range of the domain-wall mass parameter in which the chiral zero mode survives on the domain wall. In the symmetric phase ($\beta_s = 0.5$), however, such an allowed region of the domain-wall mass parameter for the chiral zero mode, if it exists, is found to be very narrow. Our conclusions and a discussion are given in Sec. IV.

II. DOMAIN-WALL MODEL

A. Definition of the model

We consider a vector gauge theory in $d = 2k + 1$ dimensions with a domain-wall mass term, which has the shape of a step function in the coordinate of an extra dimension. This domain-wall model was originally proposed by Kaplan [2], and the fermionic part of the action is reformulated by Narayanan-Neuberger [6], in terms of a $2k$ -dimensional theory. The model is defined by the action

$$S = S_G + S_F, \quad (1)$$

where S_G is the action of a dynamical gauge field and S_F is the fermionic action. S_G is given by

$$S_G = \beta \sum_{n, \mu > \nu} \sum_s \{1 - \text{Re Tr}[U_{\mu\nu}(n, s)]\} + \beta_s \sum_{n, \mu} \sum_s \{1 - \text{Re Tr}[U_{\mu d}(n, s)]\}, \quad (2)$$

where μ, ν run from 1 to $2k$, n is a $2k$ -dimensional lattice point, and s is a coordinate of an extra dimension. $U_{\mu\nu}(n, s)$ is a $2k$ -dimensional plaquette and $U_{\mu d}(n, s)$ is a plaquette containing two link variables in the extra direction. β is the inverse gauge coupling for the plaquette $U_{\mu\nu}$ and β_s is the one for the plaquette $U_{\mu d}$. In general, $\beta \neq \beta_s$. The fermion action S_F on the Euclidean lattice, in terms of the $2k$ -dimensional notation, is given by

$$S_F = \frac{1}{2} \sum_{n, \mu} \sum_s \bar{\psi}_s(n) \gamma_\mu [U_{s, \mu}(n) \psi_s(n + \mu) - U_{s, \mu}^\dagger(n - \mu) \psi_s(n - \mu)] + \sum_n \sum_{s, t} \bar{\psi}_s(n) [M_0 P_R + M_0^\dagger P_L] \psi_t(n) + \frac{1}{2} \sum_{n, \mu} \sum_s \bar{\psi}_s(n) [U_{s, \mu}(n) \psi_s(n + \mu) + U_{s, \mu}^\dagger(n - \mu) \psi_s(n - \mu) - 2 \psi_s(n)], \quad (3)$$

where s, t are an extra coordinates, $P_{R/L} = \frac{1}{2}(1 \pm \gamma_{2k+1})$ and

$$(M_0)_{s, t} = U_{s, d}(n) \delta_{s+1, t} - a(s) \delta_{s, t}, \quad (4)$$

$$(M_0^\dagger)_{s, t} = U_{s-1, d}^\dagger(n) \delta_{s-1, t} - a(s) \delta_{s, t}.$$

Here $U_{s, \mu}(n), U_{s, d}(n)$ ($d = 2k + 1$) are link variables connecting a site (n, s) to $(n + \mu, s)$ or $(n, s + 1)$, respectively. Because of a periodic boundary condition in the extra dimension, s, t run from $-L_s$ to $L_s - 1$, and $a(s)$ is given by

$$a(s) = 1 - m_0 [\text{sgn}(s + \frac{1}{2}) \text{sgn}(L_s - s - \frac{1}{2})] = \begin{cases} 1 - m_0 & (-\frac{1}{2} < s < L_s - \frac{1}{2}), \\ 1 + m_0 & (-L_s - \frac{1}{2} < s < -\frac{1}{2}), \end{cases} \quad (5)$$

where m_0 is the height of the domain-wall mass. It is easy to check that the above fermionic action is identical to the one in $2k + 1$ dimensions, proposed by Kaplan [2, 6].

In the weak coupling limit of both β and β_s , it has been shown that at $0 < m_0 < 1$ a desired chiral zero mode appears on a domain wall ($s = 0$ plane) without unwanted doublers. Because of the periodic boundary condition in the extra dimension, however, a zero mode of opposite chirality to the one on the domain wall appears on the antdomain wall ($s = L_s - 1$). Overlap between two zero modes decreases exponentially at large L_s . A free fermion propagator is easily calculated and an effective action of a $(2+1)$ -dimensional model including the gauge anomaly and the Chern-Simons term can be obtained for smooth background gauge fields [3].

The original Kaplan domain-wall models, however, have not been investigated yet *nonperturbatively*, except $\beta_s = 0$ [8, 15, 16]. The main question is whether the chiral zero mode

survives in the presence of rough gauge fields mentioned in the Introduction. To answer this question we will analyze the fate of the chiral zero mode in the weak coupling limit for β . In this limit, the gauge field action S_G is reduced to

$$S_G = \beta_s \sum_s \sum_{n,\mu} \{1 - \text{Re Tr}[V(n,s)V^\dagger(n+\mu,s)]\}, \quad (6)$$

where the link variable $U_{s,d}(n)$ in the extra direction is regarded as a site variable $V(n,s)[=U_{s,d}(n)]$. This action is identical to the one of a $2k$ -dimensional spin model and s is regarded as an independent flavor. The action (6) is invariant under

$$V(n,s) \rightarrow g(s)V(n,s)g^\dagger(s+1) \quad [g(s) \in G], \quad (7)$$

where G is the gauge group of the original model. Therefore the total symmetry of the model is G^{2L_s} , where $2L_s$, the size

of the extra dimension, is regarded as the number of independent flavors. We use this (reduced) model for our numerical investigation.

B. Mean-field approximation for fermion propagators

When the dynamical gauge fields are added even on the extra dimension only, it is difficult to calculate the fermion propagator analytically. Instead of calculating the fermion propagator *exactly*, we use a mean-field approximation to see the effect of the dynamical gauge field qualitatively. The mean-field approximation we adopt is that the link variables are replaced as

$$V(n,s)[=U_{s,d}(n)] \rightarrow z, \quad (8)$$

where z is a (n,s) -independent real constant. From Eq. (3) the fermion action in a $2k$ -dimensional momentum space becomes

$$S_F \rightarrow \sum_{s,t,p} \bar{\psi}_s(-p) \left(\sum_{\mu} i\gamma_{\mu} \sin(p_{\mu}) \delta_{s,t} + [M(z)P_R + M^\dagger(z)P_L]_{s,t} \right) \psi_t(p), \quad (9)$$

$$[M(z)]_{s,t} = [M_0(z)]_{s,t} + \frac{\nabla(p)}{2} \delta_{s,t}, \quad [M^\dagger(z)]_{s,t} = [M_0^\dagger(z)]_{s,t} + \frac{\nabla(p)}{2} \delta_{s,t}, \quad \nabla(p) \equiv \sum_{\mu=1}^{d-1} 2(\cos p_{\mu} - 1), \quad (10)$$

$$[M_0(z)]_{s,t} = z \delta_{s+1,t} - a(s) \delta_{s,t}, \quad [M_0^\dagger(z)]_{s,t} = z \delta_{s-1,t} - a(s) \delta_{s,t}. \quad (11)$$

Following Refs. [3,6] it is easy to obtain a mean-field fermion propagator on a finite lattice with periodic boundary conditions:

$$\begin{aligned} G(p)_{s,t} &= \left[i \sum_{\mu} \gamma_{\mu} \bar{p}_{\mu} + M(z)P_R + M^\dagger(z)P_L \right]_{s,t}^{-1} \\ &= \left[\left(-i \sum_{\mu} \gamma_{\mu} \bar{p}_{\mu} + M(z) \right) G_L(p)_{s,t} \right] P_L + \left[\left(-i \sum_{\mu} \gamma_{\mu} \bar{p}_{\mu} + M^\dagger(z) \right) G_R(p)_{s,t} \right] P_R, \end{aligned} \quad (12)$$

$$G_L(p) = \frac{1}{\bar{p}^2 + M^\dagger(z)M(z)}, \quad G_R(p) = \frac{1}{\bar{p}^2 + M(z)M^\dagger(z)}, \quad (13)$$

with $\bar{p}_{\mu} \equiv \sin(p_{\mu})$. For large L_s where we neglect terms of $O(e^{-cL_s})$ with $c > 0$, G_L and G_R are given by

$$\begin{aligned} [G_L(p)]_{s,t} &= \begin{cases} B e^{-\alpha_+|s-t|} + (A_L - B) e^{-\alpha_+(s+t)} + (A_R - B) e^{-\alpha_+(2L_s - s - t)} & (s, t \geq 0), \\ A_L e^{-\alpha_+s + \alpha_-t} + A_R e^{-\alpha_+(L_s - s) - \alpha_-(L_s + t)} & (s \geq 0, t \leq 0), \\ A_L e^{-\alpha_-s - \alpha_+t} + A_R e^{-\alpha_-(L_s + s) - \alpha_+(L_s - t)} & (s \leq 0, t \geq 0), \\ C e^{-\alpha_-|s-t|} + (A_L - C) e^{-\alpha_-(s+t)} + (A_R - C) e^{-\alpha_-(2L_s + s + t)} & (s, t \leq 0), \end{cases} \quad (14) \\ [G_R(p)]_{s,t} &= \begin{cases} B e^{-\alpha_+|s-t|} + (A_R - B) e^{-\alpha_+(s+t+2)} + (A_L - B) e^{-\alpha_+(2L_s - s - t - 2)} & (s, t \geq -1), \\ A_R e^{-\alpha_+(s+1) + \alpha_-(t+1)} + A_L e^{-\alpha_+(L_s - s - 1) - \alpha_-(L_s + t + 1)} & (s \geq -1, t \leq -1), \\ A_R e^{-\alpha_-(s+1) - \alpha_+(t+1)} + A_L e^{-\alpha_-(L_s + s + 1) - \alpha_+(L_s - t - 1)} & (s \leq -1, t \geq -1), \\ C e^{-\alpha_-|s-t|} + (A_R - C) e^{-\alpha_-(s+t+2)} + (A_L - C) e^{-\alpha_-(2L_s + s + t + 2)} & (s, t \leq -1), \end{cases} \quad (15) \end{aligned}$$

where

$$a_{\pm} = z \left(1 - \frac{\nabla(p)}{2} \mp m_0 \right) = z b_{\pm}, \quad (16)$$

$$\alpha_{\pm} = \operatorname{arccosh} \left[\frac{\bar{p}^2 + z^2 + b_{\pm}^2}{2z b_{\pm}} \right], \quad (17)$$

$$A_L = \frac{1}{a_+ e^{\alpha_+} - a_- e^{-\alpha_-}}, \quad A_R = \frac{1}{a_- e^{\alpha_-} - a_+ e^{-\alpha_+}}, \quad (18)$$

$$B = \frac{1}{2a_+ \sinh \alpha_+}, \quad C = \frac{1}{2a_- \sinh \alpha_-}. \quad (19)$$

The terms A_R , B , and C have no singularity for all z as $p \rightarrow 0$ in the same case of free theory. The behavior of A_L is, however, different. As $p \rightarrow 0$, A_L behaves as

$$A_L \rightarrow \frac{1}{[(1-m_0)^2 - z^2] + O(p^2)} \quad (0 < m_0 < 1-z), \quad (20)$$

$$\rightarrow \frac{4m_0^2 - [(z^2 - 1) - m_0^2]^2}{4m_0 z^2 p^2} \quad (1-z < m_0 < 1). \quad (21)$$

A critical value of the domain-wall mass that separates a region with a zero mode and a region without zero modes is $m_0^c = 1 - z$. Since the A_L term dominates for $1 - z < m_0 < 1$ in the G_L [Eq. (14)] and G_R [Eq. (15)], a right-handed zero mode appears in the $s=0$ plane and a left-handed zero mode in the $s=L_s - 1$ plane. For $0 < m_0 < 1 - z$ the right- and left-handed fermions are massive in all s planes. Since the terms $A_L(A_R)$ and $B(C)$ have almost same value in this region of m_0 , a translational-invariant term dominates in G_L and G_R in the positive (negative) s layer, so that the spectrum becomes vector like.

If $z \rightarrow 1$, the model becomes a free theory. The propagator obtained in this section agrees with the one obtained in Ref. [3]. In the opposite limit that $z \rightarrow 0$, since there is no hopping term to the neighboring layers, this model becomes the one analyzed in Ref. [15] in the case of the strong coupling limit $\beta_s = 0$, and in Ref. [16] in the case that z is identified with the vacuum expectation value of the link variables. This consideration suggests that the region where the zero modes exist becomes smaller and smaller as z ($1 - z < m_0 < 1$) approaches zero. What corresponds to z ? Boundary conditions which z satisfies are $z=1$ at $\beta_s = \infty$ and $z=0$ at $\beta_s = 0$. The most naive candidate [16] is

$$z = \langle V(n, s) \rangle. \quad (22)$$

But this is not invariant under the symmetry (7); therefore, we are not sure whether this correspondence is good or not for the fermion propagator. The other choice, which is invariant under (7), is

$$z^2 = \langle \operatorname{Tr} \operatorname{Re} \{ V(n, s) V^\dagger(n + \mu, s) \} \rangle. \quad (23)$$

If Eq. (22) is true, zero modes disappear in the symmetric phase, where $\langle V(n, s) \rangle = 0$, while, for the case of Eq. (23), the zero modes always exist in both phases, since $\langle \operatorname{Tr} \operatorname{Re} \{ V(n, s) V^\dagger(n + \mu, s) \} \rangle$ is insensitive to which phase we are in.

III. NUMERICAL STUDY OF THE (2+1)-DIMENSIONAL U(1) MODEL

A. Method of numerical calculations

In this section we numerically study the domain-wall model in 2 + 1 dimensions with a U(1) dynamical gauge field in the extra dimension. As seen from Eq. (6), the gauge field action can be identified with a two-dimensional U(1) spin model (with $2L_s$ copies). In 2 + 1 dimensions, γ matrices are Pauli-matrices, $\sigma_1, \sigma_2, \sigma_3$.

Our numerical simulation has been carried out by the quenched approximation. Configurations of U(1) dynamical gauge field are generated and fermion propagators are calculated on these configurations. The obtained fermion propagators are gauge noninvariant in general under the symmetry (7). The fermion propagator $G(p)_{s,t}$ becomes ‘‘invariant’’ if and only if $s=t$. Thus, we take the s - s layer as the propagating plane (\approx ‘‘physical space’’), and investigate the behavior of the fermion propagator in this layer.

To study the fermion spectrum, we assume a form of Eq. (12) for the fermion propagator, from which we extract G_L and G_R . We then obtain the corresponding ‘‘fermion masses’’ from $G_L^{-1}(p)$ and $G_R^{-1}(p)$ by fitting them linearly in \bar{p}^2 , since, from Eq. (13),

$$G_L^{-1} = \bar{p}^2 + M^\dagger M \rightarrow m_f^2(\text{right}) \quad (p \rightarrow 0), \quad (24)$$

$$G_R^{-1} = \bar{p}^2 + M M^\dagger \rightarrow m_f^2(\text{left}) \quad (p \rightarrow 0). \quad (25)$$

We take the following setup for two-dimensional momenta. A periodic boundary condition is taken for the first direction and the momentum in this direction is fixed on $p_1 = 0$. An antiperiodic boundary condition is taken for the second direction and the momentum in this direction is variable such as $p_2 = (2n + 1)\pi/L$, $n = -L/2, \dots, L/2 - 1$. However, special care is necessary in order to see the existence of the zero mode numerically at the *negative* s slice. In a numerical simulation on limited lattice sizes of two dimensions, for example $L \sim 10$, the fermion spectrum obtained through the above procedure at the *negative* s slice does not correspond to the correct fermion masses, due to the coarseness of the momentum resolution. In particular it is difficult to see the expected singularity caused by the zero mode. The details of this problem will be discussed later.

B. Simulation parameters

Our simulation is performed in the quenched approximation on $L^2 \times 2L_s$ lattices with $L = 16, 24, 32$ and $L_s = 16$. The coordinate s in the extra dimension runs $-16 < s < 15$. Gauge configurations are generated by the five-hit Metropolis algorithm at $\beta_s = 0.5, 1.0, 5.0$. For the thermalization the first 1000 sweeps are discarded.

The fermion propagators are calculated by the conjugate gradient method on 50 configurations separated by at least 20 sweeps, except at $\beta_s = 5.0$ on a $32^2 \times 32$ lattice where the number of configurations are 11. We take the domain-wall

mass $m_0 = 0.7, 0.8, 0.9, 0.99$ at $\beta_s = 0.5$, $m_0 = 0.3, 0.4, 0.5, 0.6, 0.9$ at $\beta_s = 1.0$, and $m_0 = 0.1, 0.2, 0.3$ at $\beta_s = 5.0$. The boundary conditions in the first and third (extra) directions are periodic and the one in the second direction is antiperiodic. The Wilson parameter r has been set to $r=1$. The fermion propagators have been investigated mainly at $s = 0, 8, 15$. These s are the layers where we put the sources. The layer at $s=0$ is the domain wall, at $s=15$, the antidomain wall, and at $s=8$, neither. At $\beta_s=0.5$ some data have been taken also at $s = -1, -8, -16$ on a $24^2 \times 32$ lattice. Errors are all estimated by the jackknife method with unit bin size.

C. Quenched phase structure

As explained before the gauge field action of our model is identical to that of the U(1) spin system in two dimensions. Therefore, there is a Kosterlitz-Thouless phase transition and this system does not have an order parameter on the infinite lattice. On the finite volume, however, we take a vacuum expectation value of link variables as an order parameter using the rotation technique:

$$V = \left\langle \left| \frac{1}{L^2} \sum_n V(n,s) \right| \right\rangle_s, \quad (26)$$

where L is the lattice size of the first and the second dimensions.

The defined vacuum expectation value V above is zero in the Kosterlitz-Thouless phase but $V > 0$ in the spin-wave phase on a finite lattice (increasing the lattice size, however, decreasing the value of V ; in the infinite lattice size, the value of V is zero for all gauge coupling). Since we are interested in the dynamics of four-dimensional theories, where the phase transition separates a symmetric phase from a broken phase, we have used this two-dimensional system on large but finite volume as a toy model of the four-dimensional real world. Therefore, in this paper, we refer to the Kosterlitz-Thouless phase as the symmetric phase and to the spin-wave phase as the broken phase. Figure 1(a) shows that, on a $16^2 \times 32$ lattice, v behaves as if it was an order parameter. From Fig. 1(b) we consider that the system is in the symmetric phase at $\beta_s = 0.5$, while in the broken phase at $\beta_s = 1.0, 5.0$.

D. Fermion spectrum in the broken phase

At $\beta_s = 1.0$ and 5.0 , the system is in the broken phase. Here we mainly discuss the result at $\beta_s = 1.0$ in detail.

We first consider the fermion spectrum on the layer at $s=0$. Figure 2 is a plot of the term corresponding to $-\sin(p_2) \cdot G_L$ and $-\sin(p_2) \cdot G_R$ as a function of p_2 at $m_0 = 0.3$ and 0.5 . (Note that we always set $p_1=0$.) This figure shows that, as p_2 goes to zero, G_L seems to diverge at $m_0 = 0.5$ but stay finite at $m_0 = 0.3$, while G_R stays finite at both m_0 . Next we show Fig. 3, which is a plot of G_L^{-1} and G_R^{-1} as a function of $\bar{p}_2^2 \equiv \sin^2(p_2)$ at $m_0 = 0.3$ and 0.5 . In the limit $p_2 \rightarrow 0$, G_R^{-1} remains nonzero at both m_0 , while G_L^{-1} vanishes at $m_0 = 0.5$. We obtain the value of m_f^2 , which can be regarded as the mass square in a two-dimensional world, by the linear fit in \bar{p}_2^2 , and plot m_f as a function of m_0 in Fig. 4. The mass of right-handed fermions, obtained from G_L^{-1} ,

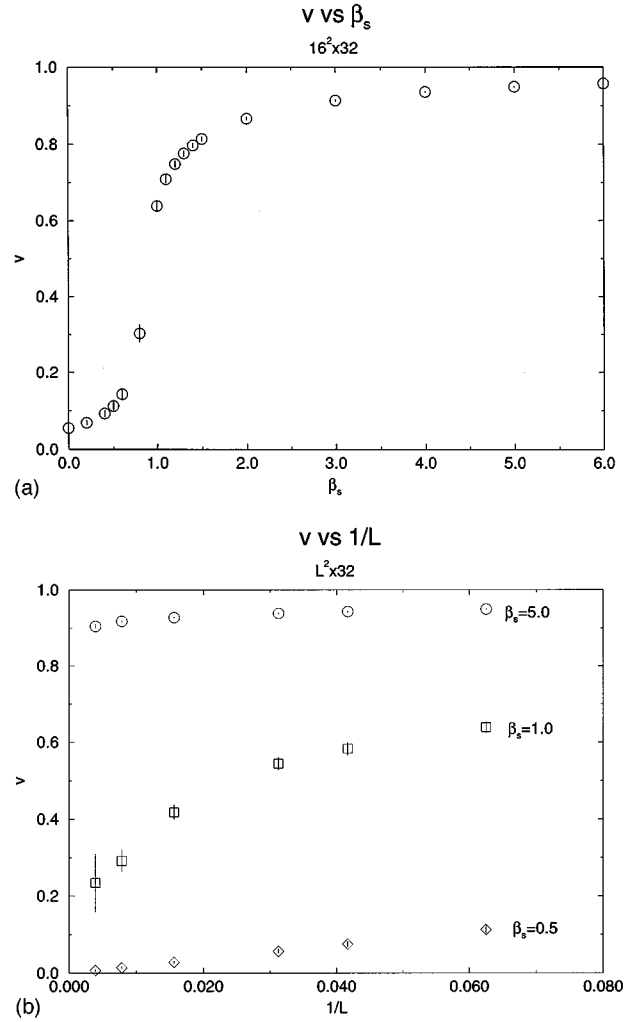


FIG. 1. (a) Vacuum expectation value of link variables V on a $16^2 \times 32$ lattice as a function of β_s . (b) Volume dependence of the vacuum expectation values of link variables V as a function of $1/L$.

becomes very small (less than 0.1) at m_0 larger than 0.5, and so we conclude that the critical value is $m_0^c \sim 0.5$. Whenever the domain-wall mass is larger than this value, this model produces a right-handed chiral zero mode on the domain wall at $s=0$.

On the antidomain wall ($s=15$), on the other hand, the mass of left-handed fermion becomes less than 0.1 at m_0 larger than the critical mass $m_0^c \sim 0.5$, as seen in Fig. 5. It is noted that chiralities between the zero modes on the domain wall and the antidomain wall are opposite each other.

Finally Fig. 6 shows that, on $s=8$, the layer in the middle between the domain wall and the antidomain wall, both right-handed and left-handed fermions stay heavy.

A similar result at $\beta_s = 5.0$ on $s=0$ is given Fig. 7.

From these results above, we conclude that the domain-wall model with the dynamical gauge field on the extra dimension (i.e., the weak coupling limit of the original Kaplan model) can create the chiral zero mode on the domain wall, at least deep in the broken phase.

Does this mean that the original Kaplan model works for the construction of lattice chiral gauge theories in the broken phase? In Ref. [8] the potential problem of the Kaplan model in the broken phase has been pointed out. Their argument is

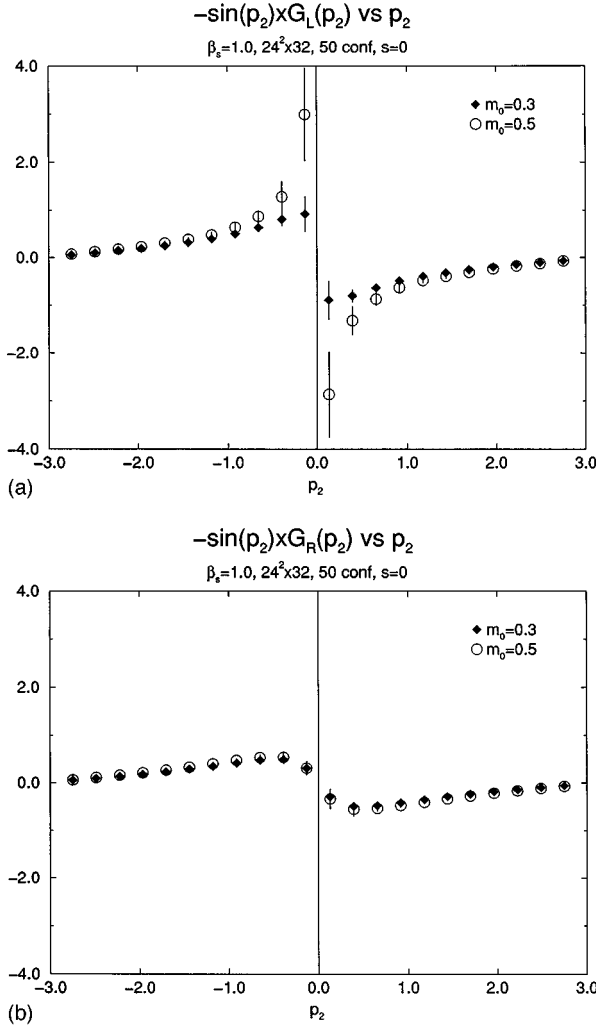


FIG. 2. $-\sin(p_2)[G_L]_{0,0}$ and $-\sin(p_2)[G_R]_{0,0}$ in the fermion propagator as a function of p_2 with $p_1=0$ at $\beta_s=1.0$ on a $24^2 \times 32$ lattice, for $m_0=0.5$ (open circles) and 0.3 (solid diamonds).

as follows: In the broken phase the symmetry group G^{2L_s} , Eq. (7), breaks down to its diagonal subgroup G , and therefore one gauge field remain massless when the physical gauge coupling is switched on. However, this massless gauge field is independent of s and couples equally to the zero modes at the domain and antdomain walls, rendering the model vector like.

We found, however, their argument should be modified slightly for a non-Abelian group G , due to the periodicity of the extra dimension. In the broken phase the vacuum expectation value of $V(n,s)$ at each layer should be

$$\langle V(n,s) \rangle = v V(s), \quad V(s) \in G. \quad (27)$$

Note that $V(s)$ can depend on s while v is an s -independent real number. In the case of $G=U(1)$ this vacuum expectation value is invariant under Eq. (7) with $g(s) = g(s+1) = g$, while such an invariant transformation does not exist in general if G is non-Abelian. Hereafter we only consider the case of $G=SU(N)$ as a concrete example,

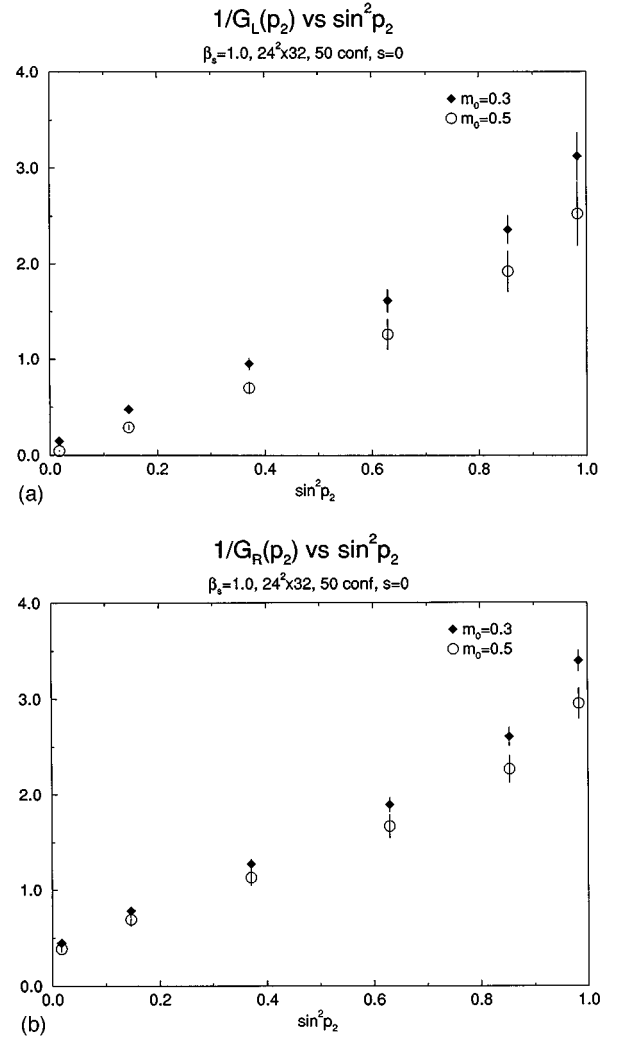


FIG. 3. $[G_L]_{0,0}^{-1}$ and $[G_R]_{0,0}^{-1}$ as a function of $\sin^2(p_2)$ with $p_1=0$ at $\beta_s=1.0$ on a $24^2 \times 32$ lattice, for $m_0=0.5$ (open circles) and 0.3 (solid diamonds).

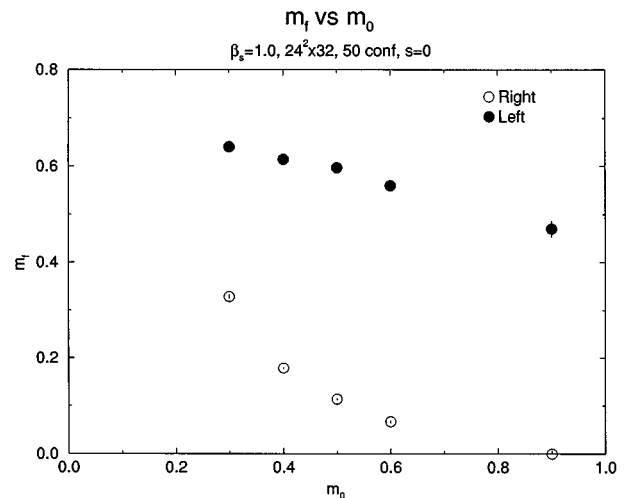


FIG. 4. m_f vs m_0 at $\beta_s=1.0$ on a $24^2 \times 32$ lattice, in the case of putting a source on the domain wall $s=0$, for the right-handed fermion (open circles) and the left-handed fermion (solid circles).

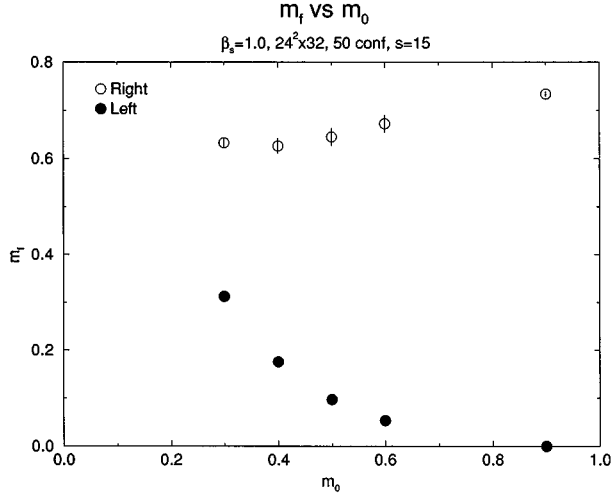


FIG. 5. m_f vs m_0 at $\beta_s=1.0$ on a $24^2 \times 32$ lattice, in the case of putting a source on the antdomain wall $s=15$, for the right-handed fermion (open circles) and the left-handed fermion (solid circles).

though an extension of our argument to general non-Abelian groups is straightforward. Let us apply the following gauge transformation to Eq. (27):

$$g(s)V(s)g^\dagger(s+1)=1 \quad (28)$$

for $s=-L_s, -L_s+1, \dots, L_s-3, L_s-2$, which implies

$$g(-L_s)\left(\prod_{s=-L_s}^{L_s-2} V(s)\right)g^\dagger(L_s-1)=1. \quad (29)$$

For $s=L_s-1$, the gauge transformation applied to Eq. (27) becomes

$$g(L_s-1)V(L_s-1)g^\dagger(L_s)=g(-L_s)\left(\prod_{s=-L_s}^{L_s-1} V(s)\right)g^\dagger(L_s). \quad (30)$$

Since $g(L_s)=g(-L_s)$ from the periodicity of the extra dimension, there exists a gauge transformation $g_0=g(L_s)=g(-L_s)$ such that

$$g_0\left(\prod_{s=-L_s}^{L_s-1} V(s)\right)g_0^\dagger=D, \quad (31)$$

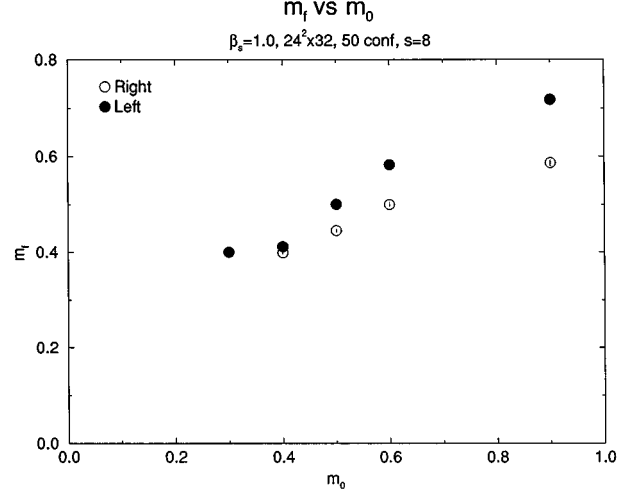


FIG. 6. m_f vs m_0 at $\beta_s=1.0$ on a $24^2 \times 32$ lattice, in the case of putting a source on $s=8$, for the right-handed fermion (open circles) and the left-handed fermion (solid circles).

where D is a diagonal matrix: $D_{ab}=e^{i\theta_a}\delta_{ab}$ with $\sum_{a=1}^N \theta_a \equiv 0 \pmod{2\pi}$. If this D belongs to a center of G [Z_N for $SU(N)$], the transformed vacuum expectation value $\langle V(n,s) \rangle = v$ for $s \neq L_s-1$ and $=vD$ for $s=L_s-1$ is invariant under further constant gauge transformations, $g(s)=g$. In this case the conclusion of Ref. [8] is valid. Since the dynamics of $V(n,s)$ is completely independent at each layer for the quenched case, however, there is no special reason that D belongs to the center of G ; therefore, probability having $D \in Z_N$ out of $SU(N)$ is (almost) zero. In the presence of dynamical fermions, we cannot rule out the possibility that $D \in Z_N$ is always satisfied dynamically. But, since $v^{2L_s} \text{Tr} D = v^{2L_s} \text{Tr} \prod_{s=-L_s}^{L_s-1} V(s) = \text{Tr} \prod_{s=-L_s}^{L_s-1} \langle U_{s,d}(n) \rangle$ is the Polyakov loop in the extra dimension, it should depend on parameters such as β_s and m_0 , and it is unlikely that $D \in Z_N$ is always satisfied, irrespective of values of such parameters. Thus, hereafter, we assume $D \notin Z_N$.

Next let us consider the effect of $D \notin Z_N$ to the would-be gauge boson mass terms:

$$S_G^{\text{mass}} = \beta_s \sum_{n,\mu} \sum_s \{1 - \text{Re} \text{Tr}[U_\mu(n,s)V(n+\mu,s)U_\mu^\dagger(n,s+1)V^\dagger(n,s)]\}. \quad (32)$$

Replacing $V(n,s) \rightarrow \langle V(n,s) \rangle = vV(s)$, we obtain

$$S_G^{\text{mass}} = \beta_s v^2 \sum_{n,\mu} \left\{ \sum_{s=-L_s}^{L_s-2} [1 - \text{Re} \text{Tr}\{\tilde{U}_\mu(n,s)\tilde{U}_\mu^\dagger(n,s+1)\}] + [1 - \text{Re} \text{Tr}\{\tilde{U}_\mu(n,L_s-1)D\tilde{U}_\mu^\dagger(n,L_s)D^\dagger\}] \right\}, \quad (33)$$

where $\tilde{U}_\mu(n,s) = g(s)U_\mu(n,s)g^\dagger(s)$. Expanding $\tilde{U}_\mu(n,s) = \exp[igA_\mu(n,s)]$ up to $O(A_\mu^2)$ we obtain

$$S_G^{\text{mass}} = \beta_s v^2 \frac{g^2}{2} \sum_{n,\mu} \left[\sum_{s=-L_s}^{L_s-1} \text{Tr} \{ A_\mu(n,s) - A_\mu(n,s+1) \}^2 - 2 \text{Tr} \{ A_\mu(n,L_s-1) D A_\mu(n,L_s) D^\dagger - A_\mu(n,L_s-1) A_\mu(n,L_s) \} \right]. \quad (34)$$

For the gauge field constant on the extra dimension,

$$S_G^{\text{mass}} = -\beta_s v^2 g^2 \sum_{n,\mu} A_\mu^a(n) A_\mu^b(n) \text{Tr} [T^a D T^b D^\dagger - T^a T^b] \quad (35)$$

and

$$S_G^{\text{kin}} \propto -\beta g^2 2L_s \sum_{n,\mu\nu} F_{\mu\nu}^2(n). \quad (36)$$

Since $\text{Tr} [T^a D T^b D^\dagger - T^a T^b] = 0$ for $N-1$ diagonal generators T^a of $SU(N)$ (note that $DD^\dagger = 1$), there are $N-1$ massless gauge fields constant on the extra dimension, which couples equally to the zero modes at the domain and antidomain walls. These generators form a subgroup of G , denoted H . The remaining $(N-1)N$ gauge fields have nonzero mass: $m_G^2 \propto \beta_s v^2 / \beta 2L_s$, which controls propagation of these gauge fields at a given s slice.

The above consideration shows that the symmetry G^{2L_s} breaks down to H in the broken phase, if L_s is finite. Since an overlap between the zero modes at the domain and antidomain walls is suppressed exponentially in L_s , there is a window of L_s values where the chiral zero mode exists and masses of the gauge fields, which correspond to $G-H$ generators, are nonzero. Therefore, deep in the broken phase, Kaplan's model can describe, at best, a chiral fermion interacting with the gauge fields of $G-H$ generators at a finite cutoff, if L_s is appropriately chosen. In the scaling limit ($v \rightarrow v_R a$), however, there exist two problems. One is that the constant gauge fields of $G-H$ generators have finite masses in this limit and thus appear in the continuum spectrum, since $m_G^2 \propto \beta_s v_R^2 / \beta 2L_s$. How serious the effect of

these gauge bosons to the chiral zero mode is depends on how they propagate not only in space-time at a given s slice but also in the extra dimension. Formula Eq. (34) suggests that the propagation in the extra dimension is suppressed by another ‘‘mass,’’ which is independent of both v and L_s . A detail analysis of this point, however, needs a nonperturbative simulation with the physical gauge fields and thus is beyond the scope of this paper. The other problem is the fermion spectrum in the limit. If the fermion spectrum stays chiral in the limit, it should stay chiral also in the symmetric phase. This means that, in order to determine the fermion spectrum in the scaling limit from the broken phase, we have to know the spectrum in the symmetric phase. Therefore, from knowledge of the fermion spectrum obtained in the broken phase so far, we cannot draw any conclusion on the fermion spectrum, chiral or vector like, in the scaling limit.

E. Fermion spectrum in the symmetric phase

The system is in the symmetric phase at $\beta_s = 0.5$. The fermion propagator is analyzed in the same way as in the broken phase. However, for example, on the $s=0$ layer, $-\sin(p_2)G_L$ and $-\sin(p_2)G_R$ show similar behaviors on a $16^2 \times 32$ lattice, as seen in Fig. 8. Smaller lattice sizes show a stronger similarity, which makes analysis more difficult in the symmetric phase. To see the difference between the right-handed and left-handed fermions, we have to take a larger lattice size such as $L=24, 32$.

In Fig. 9, we have plotted the mass m_f of both modes at $s=0$ as a function of m_0 . Although the difference of masses between the right-handed and the left-handed fermions is very small, about 0.1 or less at $m_0=0.99$, this difference stays finite as we increase the spatial lattice size L from 24 to 32. Therefore, at the present sizes of lattices, $L=24$ and 32,

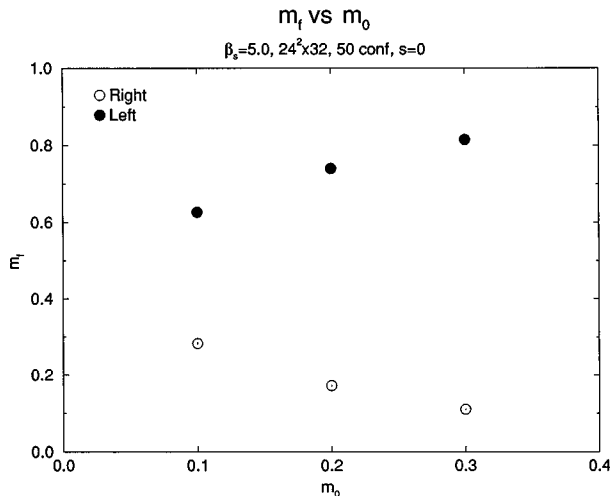


FIG. 7. m_f vs m_0 at $\beta_s = 5.0$ on a $24^2 \times 32$ lattice, in the case of putting a source on the domain wall $s=0$, for the right-handed fermion (open circles) and the left-handed fermion (solid circles).

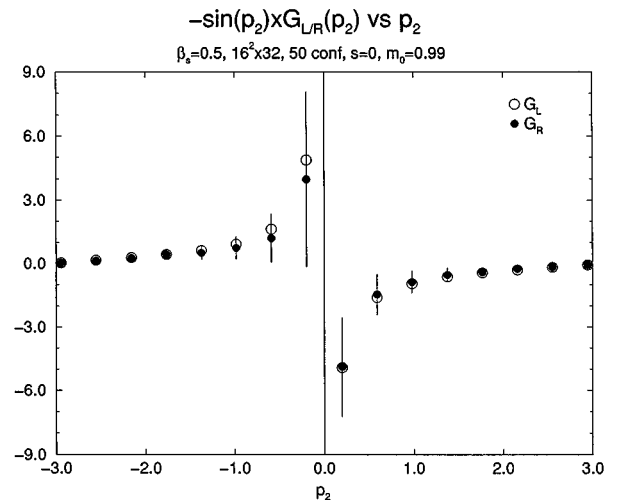


FIG. 8. $-\sin(p_2)[G_L]_{0,0}$ (open circles) and $-\sin(p_2)[G_R]_{0,0}$ (solid circles) as a function of p_2 with $p_1=0$ at $\beta_s=0.5$ on a $16^2 \times 32$ lattice.

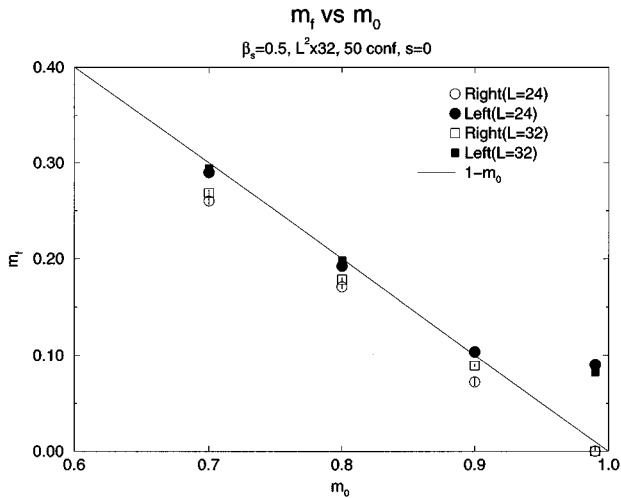


FIG. 9. m_f vs m_0 at $\beta_s=0.5$ on $L^2 \times 32$ lattices with $L=24$ (circles) and 32 (squares) in the case of putting a source on the domain wall $s=0$. Open symbols stand for the right-handed fermion and solid symbols for the left-handed fermion. The solid line corresponds to $1 - m_0$.

it seems that the right-handed fermion becomes massless at m_0 larger than 0.9, while the left-handed fermion stays massive at all m_0 , so that the fermion spectrum on the domain wall is *chiral*.

In order to see that the difference of mass between the right and the left is really a signal, not a statistical fluctuation, we have plotted m_f vs m_0 in the case of putting a source at the antdomain wall $s=15$ in Fig. 10. We observe, at $m_0=0.99$, a massless fermion of the opposite chirality to the $s=0$ zero mode and a finite difference of masses between the right and the left, which stays finite as we increase the spatial lattice size.

Furthermore, in the case of $s=8$, the right-handed fermion and the left-handed fermion stay massive at all m_0 , as seen in Fig. 11.

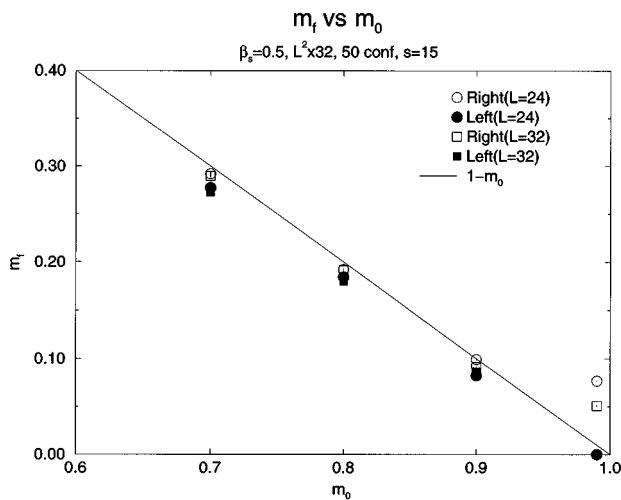


FIG. 10. m_f vs m_0 at $\beta_s=0.5$ on $L^2 \times 32$ lattices with $L=24$ (circles) and 32 (squares) in the case of putting a source on the antdomain wall $s=15$. Open symbols stand for the right-handed fermion and solid symbols for the left-handed fermion. The solid line corresponds to $1 - m_0$.

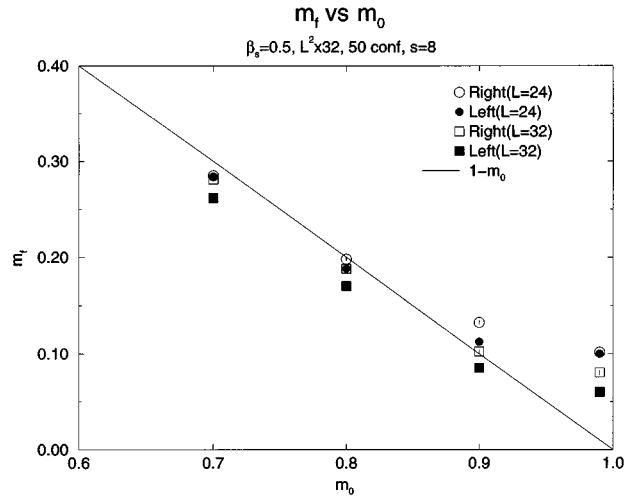


FIG. 11. m_f vs m_0 at $\beta_s=0.5$ on $L^2 \times 32$ lattices with $L=24$ (circles) and 32 (squares) in the case of putting a source on $s=8$. Open symbols stand for the right-handed fermion and solid symbols for the left-handed fermion. The solid line corresponds to $1 - m_0$.

One may wonder whether the above results could be explained by the behaviors of free Wilson fermion in the layered phase. The predicted behavior of the fermion mass in that case is $m_f=1 - m_0$ for $s \geq 0$, which gives a straight line in the above three figures, and $m_f=1 + m_0$ for $s < 0$. At first sight, our data seem to be consistent with $m_f=1 - m_0$ behavior. However, if we look at our data more closely, the data cannot be explained by $m_f=1 - m_0$, in particular, at large m_0 , and are more consistent with the existence of zero modes at large m_0 , as explained above. Furthermore, we have calculated fermion masses at a negative s slice. In Figs. 12–14 we have plotted m_f as a function of m_0 at $s=-1$, $s=-16$, and $s=-8$, respectively. If it were in the layered phase, it is expected that these data are on or near of the straight line $m_f=1 + m_0$ of a free Wilson fermion and the masses of the left-handed part and right-handed part are

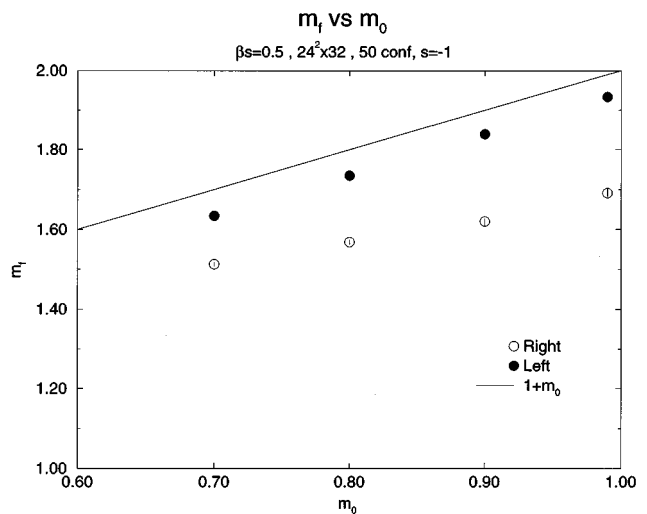


FIG. 12. m_f vs m_0 at $\beta_s=0.5$ on $24^2 \times 32$ lattices in the case of putting a source on the domain wall $s=-1$. Open symbols stand for the right-handed fermion and solid symbols for the left-handed fermion. The solid line corresponds to $1 + m_0$.

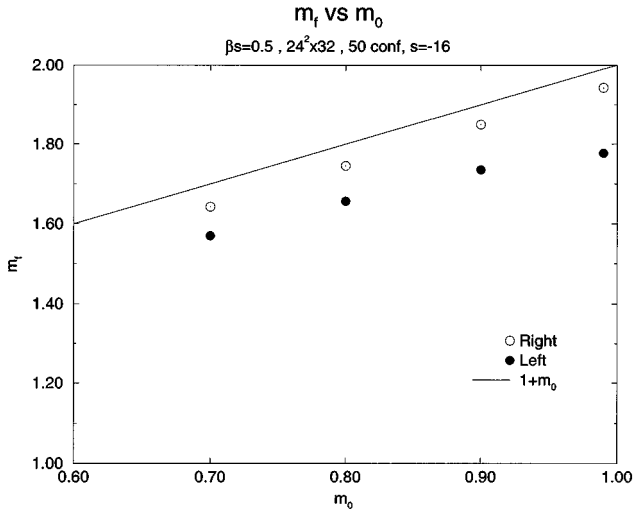


FIG. 13. m_f vs m_0 at $\beta_s=0.5$ on $24^2 \times 32$ lattices in the case of putting a source on the antidomain wall $s=-16$. Open symbols stand for the right-handed fermion and solid symbols for the left-handed fermion. The solid line corresponds to $1+m_0$.

equal particularly. Data, however, disagree with the behavior $m_f=1+m_0$ of a free Wilson fermion in the layered phase. The results at $s=-1$ and $s=-16$ differ not only from $m_f=1+m_0$ but also from the fact that the masses of the left-handed part and right-handed part are equal. Although the signal of zero modes at a negative s slice cannot be found, the observed behaviors can be qualitatively explained by Eqs. (14) and (15) of the mean-field propagator.

Neglecting the term $O(e^{-30\alpha_-})$ in Eqs. (14) and (15) we obtain

$$[G_L(p)]_{ss} = \begin{cases} C + (A_L - C)e^{-2\alpha_-}, & s = -1, \\ A_R, & s = -16, \\ C, & s = -8, \end{cases} \quad (37)$$

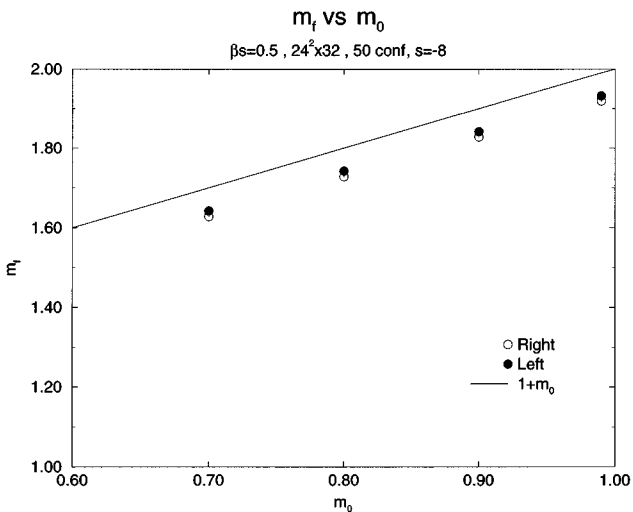


FIG. 14. m_f vs m_0 at $\beta_s=0.5$ on $24^2 \times 32$ lattices in the case of putting a source on $s=-8$. Open symbols stand for the right-handed fermion and solid symbols for the left-handed fermion. The solid line corresponds to $1+m_0$.

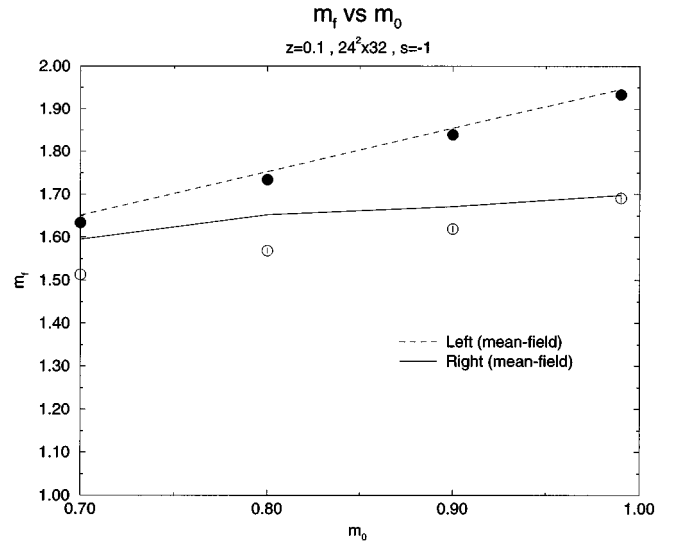


FIG. 15. m_f vs m_0 , obtained by the mean-field propagators with $z=0.1$ on $24^2 \times 32$ lattices in the case of putting a source on the domain wall $s=-1$. The solid line stands for the right-handed fermion and dashed line for the left-handed fermion. Data at $\beta_s=0.5$ (open symbols and solid symbols) are given for comparison.

$$[G_R(p)]_{ss} = \begin{cases} A_R, & s = -1, \\ C + (A_L - C)e^{-2\alpha_-}, & s = -16, \\ C, & s = -8, \end{cases} \quad (38)$$

which predict $m_f(\text{right}) = m_f(\text{left})$ at $s=-8$ and $m_f(\text{right}) \neq m_f(\text{left})$ at $s=-1$ and -16 . This behavior is qualitatively consistent with our data. However, the resolution of momentum at the current lattice size, $L=24$, is too coarse to see the expected singularity of A_L at a negative s slice, since numerically $|C| \gg |(A_L - C)e^{-2\alpha_-}|$ for $p_1=0$ and $p_2=\pi/L$ with $L=24$. For example we have calculated m_f applying the same analysis to the mean-field propagators $[G_L(p)]_{ss}$ and $[G_R(p)]_{ss}$ with a given z at $s=-1$ and $L=24$. In Fig. 15 we have plotted m_f as a function of m_0 with $z=0.1$ together with our data of m_f in Fig. 12. Even if the singularity in A_L exists the sign of this cannot be seen both the numerical simulation and the mean-field propagator at the two-dimensional lattice size $L \sim 10$.

Next we try to fit G_L^{-1} and G_R^{-1} at a given m_0 using the form of the mean-field propagator, Eqs. (14) and (15), with the fitting parameter z . In Fig. 16 we have plotted z obtained by the fit as a function of m_0 at $s=0$ on $24^2 \times 32$ and $32^2 \times 32$ lattices, and the z is almost independent of m_0 or lattice sizes. This result shows that fermion propagators obtained by the numerical simulation are consistent with the form of the mean-field propagators with small $z \approx 0.1$.

In summary our results of m_f at both positive s and negative s planes favor more the existence of a chiral zero mode in the symmetric phase than the realization of the layered phase on $L^2 \times 32$ lattices with $L=24$ and 32 . However, the possibility of it being in the layered phase is not denied. If we assume the form of the mean-field propagator, the value of the corresponding z is small, about 0.1 , at $\beta_s=0.5$, and this may suggest that the identification that $z = \langle V(n, s) \rangle$, Eq.

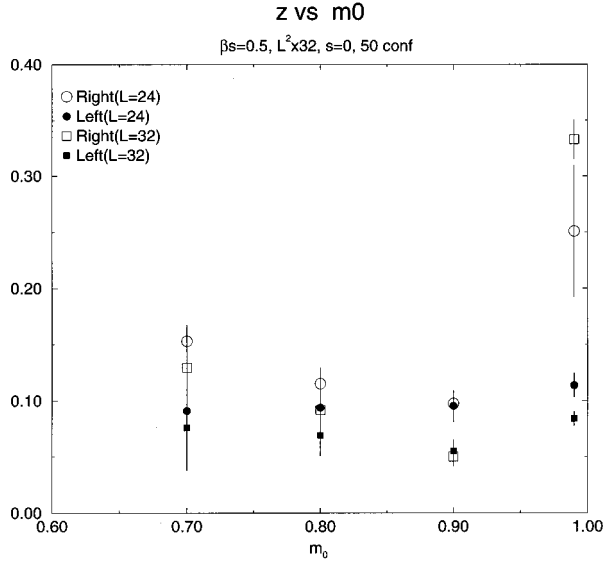


FIG. 16. z vs m_0 at $\beta=0.5$ on $L^2 \times 32$ lattices with $L=24$ (circles) and $L=32$ (squares), in the case of putting a source on the domain wall $s=0$. Open symbols stand for the right-handed fermion and solid symbols for the left-handed fermion.

(22), may be correct. If so, the layered phase will emerge in the infinite volume limit, and thus, the original Kaplan model fails to describe lattice chiral gauge theories in the symmetric phase. Unfortunately, since our data do not change very much from $L=24$ to 32 and in the infinite volume there does not exist an order parameter due to reducing the $(2+1)$ -dimensional $U(1)$ gauge system to the two-dimensional $U(1)$ spin model, so far we cannot conclude what will be the fate of chiral zero modes in the infinite volume limit.

IV. CONCLUSIONS AND DISCUSSION

Using the quenched approximation, we have performed a numerical study of the domain-wall model in $2+1$ dimensions with the $U(1)$ dynamical gauge field on the extra di-

mension. From this study we obtain the following results. In the broken phase of the gauge field, there exists a critical value of the domain-wall mass separating the region with a chiral zero mode and the region without it. At a domain-wall mass larger than its critical value a zero mode with one chirality exists on the domain wall and a zero mode with opposite chirality on the antdomain wall, and none in the middle between the domain wall and the antdomain wall. Although our data in the symmetric phase on $L^2 \times 32$ with $L=24$ and 32 suggest the existence of zero modes at $m_0=0.99$, the existence of zero modes in the symmetric phase is not conclusive for very large L . This is because our data may well be explained by the mean-field propagator with a very small z , less than 0.1 , and this small z may suggest $z = \langle V(n,s) \rangle$, which could be nonzero on the finite lattices. If so, the zero modes in the symmetric phase would disappear and the layered phase would emerge in the infinite volume limit.

The existence of chiral zero modes in the symmetric phase is essential for the original domain-wall model working as lattice chiral gauge theories. We will have to make a definite conclusion on this point. However, in $2+1$ dimensions, it seems very difficult to prove or disprove the existence of zero modes in the symmetric phase since it requires a very large L . Instead of investigating the model in $2+1$ dimensions at large L , for example $L=512$ or 1024 , we are planning to study realistic $(4+1)$ -dimensional models with $U(1)$ or $SU(N)$ gauge fields in the $\beta=\infty$ limit. Such models in the $\beta=\infty$ limit have a phase transition characterized by an order parameter, a vacuum expectation value of the link variables in the extra dimension. We hope that the finite size scaling study in the model can lead to a definite conclusion on the existence of zero modes in the symmetric phase.

ACKNOWLEDGMENTS

Numerical calculations for the present work have been carried out at the Center for Computational Physics, University of Tsukuba. This work was supported in part by the Grants-in-Aid of the Ministry of Education (Nos. 04NP0701, 06740199).

-
- [1] H. B. Nielsen and M. Ninomiya, Nucl. Phys. **B185**, 20 (1981); **B193**, 173 (1981); Phys. Lett. **105B**, 219 (1981); L. H. Karsten, Phys. Lett. **104B**, 315 (1981).
 [2] D. B. Kaplan, Phys. Lett. B **288**, 342 (1992).
 [3] S. Aoki and H. Hirose, Phys. Rev. D **49**, 2604 (1994).
 [4] K. Jansen, Phys. Lett. B **288**, 348 (1992).
 [5] M. F. L. Golterman, K. Jansen, and D. B. Kaplan, Phys. Lett. B **301**, 219 (1993).
 [6] R. Narayanan and H. Neuberger, Phys. Lett. B **302**, 62 (1993).
 [7] R. Narayanan and H. Neuberger, Nucl. Phys. **B412**, 574 (1994).
 [8] M. F. L. Golterman, K. Jansen, D. N. Petcher, and J. C. Vink, Phys. Rev. D **49**, 1606 (1994).
 [9] M. F. L. Golterman and Y. Shamir, Phys. Rev. D **51**, 3026 (1995).
 [10] R. Narayanan and H. Neuberger, Nucl. Phys. **B443**, 305 (1995); R. Narayanan, H. Neuberger, and P. Vranas, Phys. Lett. B **353**, 507 (1995); S. Randjbar-Daemi and J. Strathdee, Nucl. Phys. **B443**, 386 (1995); T. Kawano and Y. Kikukawa, Report No. KUNS-1317, 1995 (unpublished).
 [11] S. Aoki and R. B. Levien, Phys. Rev. D **51**, 3790 (1995).
 [12] Y. Shamir, Nucl. Phys. **B417**, 167 (1994).
 [13] M. F. L. Golterman and Y. Shamir, Phys. Lett. B **353**, 84 (1995); Report No. WASH-U-HEP-95-62, 1995 (unpublished).
 [14] R. Narayanan and H. Neuberger, Phys. Lett. B **388**, 303 (1995).
 [15] H. Aoki, S. Iso, J. Nishimura, and M. Oshikawa, Mod. Phys. Lett. A **9**, 1755 (1994).
 [16] C. P. Korthals-Altes, S. Nicolis, and J. Prades, Phys. Lett. B **316**, 339 (1993).